Social forces for team coordination in ball possession game

Keiko Yokoyama,[1,*] Hiroyuki Shima,[2] Keisuke Fujii,[3] Noriyuki Tabuchi,[4] and Yuji Yamamoto[1]

[1]*Research Center of Health, Physical Fitness & Sports, Nagoya University, Furo-cho, Chikusa-ku, Nagoya, 464-8601, Japan*

[2]*Department of Environmental Sciences, University of Yamanashi, 4-4-37 Takeda, Kofu, Yamanashi, 400-8510, Japan*

[3]*Center for Advanced Intelligence Project, Institute of Physical and Chemical Research (RIKEN) 6-2-3, Furuedai, Suita, Osaka, 565-0874, Japan*

[4]*Mizuno Corporation, 1-12-35 Nanko Kita, Suminoe-ku, Osaka, 559-8510, Japan*

(Received 14 April 2017; revised manuscript received 11 December 2017; published 20 February 2018)

Team coordination is a basic human behavioral trait observed in many real-life communities. To promote teamwork, it is important to cultivate social skills that elicit team coordination. In the present work, we consider which social skills are indispensable for individuals performing a ball possession game in soccer. We develop a simple social force model that describes the synchronized motion of offensive players. Comparing the simulation results with experimental observations, we uncovered that the cooperative social force, a measure of perception skill, has the most important role in reproducing the harmonized collective motion of experienced players in the task. We further developed an experimental tool that facilitates real players' perceptions of interpersonal distance, revealing that the tool improves novice players' motions as if the cooperative social force were imposed.

DOI: 10.1103/PhysRevE.97.022410

I. INTRODUCTION

Team coordination is a self-organization process observed in collective human behavior [1–3], through which members of a team operate efficiently in pursuit of their specified tasks. In most cases, a high degree of team coordination is necessary for smooth functioning of any real-life community, such as a rescue party, company, or government. The effects of team coordination are expressed by the fact that an "expert team" may not be equivalent to a "team of experts"; namely, the performance of a team as a whole can be superior to the sum of individual performances of the team members. In addition, excellent team coordination is attained only if members secure maximum efficiency while minimizing their effort. To achieve excellence in team coordination, it is important in general for members to be acutely conscious of their common goal, because it facilitates active interactions, information sharing, and strategy development.

Collective sports are a familiar example of human activities that demand a high degree of team coordination. In fact, collective sports have long been considered an optimal testing ground to understand human collective behavior; players on a team share the common goal of winning, while individual movements are regulated using sophisticated rules established throughout the vast length of human history [4–11]. Recent studies have suggested that the network dynamics of passing a ball in soccer [12] and the role-switching behavior of a defensive team in basketball [13] demonstrate the significance of excellent team coordination. In particular, the study of a ball possession task among three persons [14] revealed a spatio-temporal synchronization in players' movements similar to those occurring in coupled biological oscillators of slime molds [15] or arrays of candle-flame oscillations [16]. The most salient finding reported in Ref. [14] is the existence of variety in synchronized modes [17]. Furthermore, the various modes that occur were found to depend on the proficiency level of the triad; experienced teams commonly showed a specific class of synchronized mode, while novice teams fell into another specific class of synchronized mode in their collective motion. The direct correlation between the observed synchronized mode and the performance level of the triad may allow us to infer the interpersonal skill that promotes degree of team coordination. To proceed with this consideration, it is essential to understand the interaction mechanism used by experienced players to elevate their team's performance.

The concept of "social force" [18] provides a way of thinking about the interpersonal interaction mechanism, along with the traditional psychological [3,19] and neuroscience-based [20,21] approaches. A social model adopts the sociopsychological perspective suggested by Lewin [22], in which individual behavioral changes are guided by social fields or social forces. Social force is not an ordinary type of force exerted by a physical object, but rather a quantity that indicates a player's motivation to react to perceived information he or she obtains from an external environment [18,23–25]. In the present work, we develop a social force model that reproduces the synchronized behavior observed in the three versus one ball possession task in soccer. The model involves three kinds of social forces acting on players; among the three forces, the one called "cooperative force" [see Eq. (5)] turned out to have a crucial role in successful reproduction of the synchronized behavior associated with experienced players. The simulation results are consistent in quality with behavioral experiment data, suggesting that the social force-based approach gives a clue to determination of the fundamental social skills needed to bring about excellent team coordination in collective sports.

*Corresponding author: yokoyama@htc.nagoya-u.ac.jp

 ©2018 American Physical Society

II. EMPIRICAL DATA

To analyze team coordination, we focus on pass coordination in soccer as a three versus one ball possession task [Fig. 1(a)]. This task is often used to develop team coordination skills on a sports field. Among the four participants, three offensive players were instructed to pass a ball to each other as many times as possible, while one defensive player was instructed to intercept the ball as soon as possible. During the task, the three offensive players attempted to exchange the ball by passing it to their teammates in a limited area while avoiding ball interceptions by the defending player.

Figure 1 shows a snapshot of the ball possession task [Fig. 1(a)] and the empirical data obtained by our behavioral measurement [Figs. 1(b) and 1(c)]; a portion of this was duplicated from our previous study [14]. The measurement involved 32 subjects, which comprised a group of 16 experienced players and that of 16 novice players (19–21 years old). Each of the two groups was divided into four subgroups of four players. Every subgroup was asked to play the ball possession task for 90 sec in one trial, with four trials per subgroup. For each trial, a different person in a given subgroup took the role of the defensive player. This means that the skill levels among the three offensive players and one defensive player were almost equal. The movement of the players was recorded using a video camera (Sony HDRXR550V) at 30 frames per second. The positions of the players in the play area were extracted using the direct linear transformation method for a two-dimensional reconstruction of the images.

Spatio-temporal synchronization in offensive players was explored by probing time evolution in the three inner angles of the triangle constructed by the triad, as designated by θ_i ($i = 1,2,3$) in Fig. 1(a). Figure 1(b) presents the time variation in θ_i for experienced and novice players. It follows from the upper panel in Fig. 1(b) that experienced players tended to maintain an equilateral triangle with slight fluctuations. This result implies that experienced players regulated their relative positions during the task while maintaining all the θ_i at nearly $\pi/3$, as a result of which the pass course (i.e., an edge of the triangle) was as far from the defensive player as possible. In contrast, novice players showed significant deviation from the equilateral triangle during the task, as demonstrated in the bottom panels in Fig. 1(b). The most important observation was that the difference in team coordination between experienced and novice players was highlighted by the difference in the occurrence frequency of synchronized patterns among inner three angles [14]. Figure 1(c) illustrates the two typical synchronized patterns deduced from the behavioral measurement. The one is called the rotation (R) pattern, in which three inner angles are synchronized with a phase difference $\cong 2\pi/3$. The other is called the partial antiphase (PA) pattern, in which two angles are synchronized with a phase difference $\cong \pi$ as an antiphase manner while the remaining one is kept constant. The bottom panels in Fig. 1(c) illustrate the criteria for evaluating the synchronized patterns, in which a $\pm\pi/6$ angle margin was set when calculating the phase difference. We found that experienced players tended to yield the R pattern, whereas novice players did the PA pattern. These empirical data provide us with criteria to examine team coordination in the ball possession task.

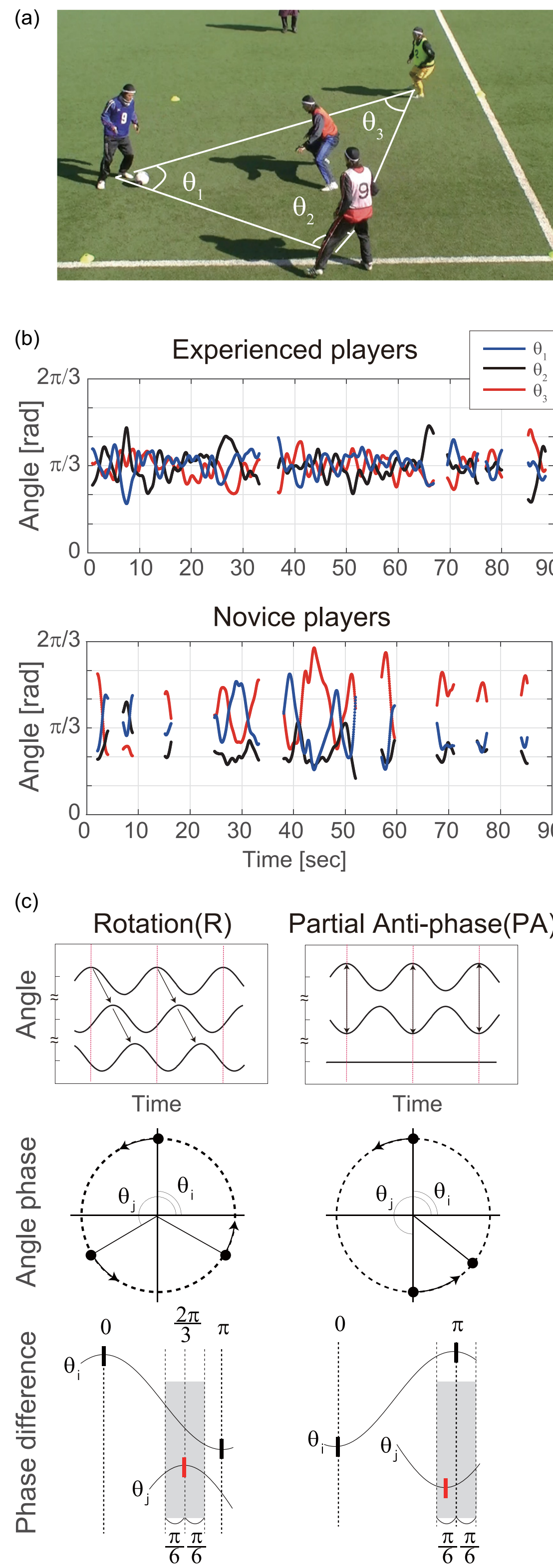

FIG. 1. Empirical data of the three versus one ball possession task [14]. (a) Snapshot of four players during the task. The definitions of the angle parameters (θ_1, θ_2, and θ_3) are illustrated in the image. (b) Time evolution in the three inner angles of the team composed of experienced and novice players. The blank periods in the time series indicate a pause resulting from ball interceptions by the *Defender*. (c) Schematic diagram of the two specific synchronized patterns: the rotation (R) and the partial antiphase (PA) pattern.

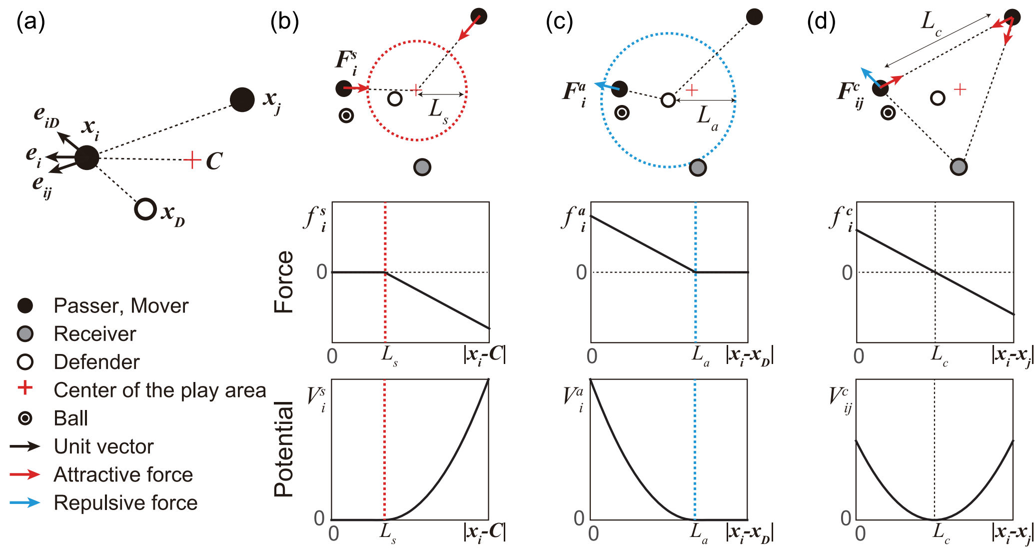

FIG. 2. (a) Schematic definitions of position vectors and unit vectors used in the simulation. (b–d, top) Diagram of three social forces acting on player i. (b) The spatial force is depicted by red arrows. This force acts only when the offensive agent is outside the circle with a radius of the spatial range parameter, L_s (shown by a red dashed circle). (c) The avoiding force is depicted by blue arrows. This force acts only when the offensive agent is inside the *Defender*-centered circle with a radius of the avoiding range parameter, L_a (shown by the blue dashed circle). (d) The cooperative force acting on the pairs of offensive agents. When the distance is larger (or smaller) than the cooperative range parameter, L_c, it exerts an attractive (repulsive) force on the pair. (b–d, middle and bottom) Spatial profiles of the social forces and associated potential fields. f_i^s, f_i^a, and f_i^c indicate the respective projections of the force vectors F_i^s, F_i^a, and F_i^c. See the main text for the precise mathematical definitions of the three social forces.

III. SOCIAL FORCE

A. Spatial, avoiding, and cooperative forces

We now demonstrate that the movement of the players observed in the experiment can be described using a social force model [18]. Our model comprises four self-driven agents with different roles, labeled *Passer*, *Receiver*, *Mover*, and *Defender*. The first three are offensive agents: the *Passer* passes the ball to the *Receiver*, while the *Mover* moves freely or proactively in preparation for a successive role switch. The *Defender* tries to intercept the ball by blocking the pass and capturing it. We assume that the roles of the offensive agents alter in a cyclic manner when the *Receiver* touches the ball passed by the *Passer*. The rotational direction of role switching is set to be random, changing stochastically from clockwise to counterclockwise and vice versa. This randomized passing direction reflects the fact that in real behavioral experiments players chose the passing direction arbitrarily.

We hypothesize that the movements of the *Passer* and *Mover* are governed by social forces, because they must adjust their motions in response to social information perceived from the environment (e.g., their relative positions to other players and to the outer boundary of the play area). In contrast, the *Receiver* is free from any social force since he or she always chases the ball regardless of environmental changes; this issue is revisited in an appendix. The equation of motion for the *Passer* and *Mover* is defined by

$$m_i \frac{d\boldsymbol{v_i}}{dt} = \boldsymbol{F}_i = \boldsymbol{F}_i^s + \boldsymbol{F}_i^a + \sum_{(j\neq i)} \boldsymbol{F}_{ij}^c, \quad i \in \{P,M\}, j \in \{P,M,R\}. \tag{1}$$

Here $\boldsymbol{F}_i^s$ is the spatial force that attracts agent i to the center of the play area. It represents the psychological motivation of the agent to stay within the play area surrounded by a circular boundary. $\boldsymbol{F}_i^a$ is the avoiding force that repulses agent i from the *Defender*. This force is a measure of the extent to which the agent perceives psychological pressure from the *Defender*. $\boldsymbol{F}_{ij}^c$ is the cooperative force that attracts or repulses agent i to or from agent j. This force reflects the tendency of experienced offensive agents to maintain close distance between each other during the task to enhance the accuracy of ball manipulation and reduce the amount of effort. m_i and $\boldsymbol{v_i}$ in Eq. (1) are the mass and velocity of agent i.

The magnitudes of the three forces are assumed to depend on the spatial configuration of the agents involved, as described below. First, the spatial force $\boldsymbol{F}_i^s$ is defined by

$$\boldsymbol{F}_i^s = \begin{cases} -k_s(|\boldsymbol{x}_i - \boldsymbol{C}| - L_s)\boldsymbol{e}_i, & \text{if } |\boldsymbol{x}_i - \boldsymbol{C}| \geqslant L_s, \\ \boldsymbol{0}, & \text{otherwise} \end{cases} \tag{2}$$

with

$$\boldsymbol{e}_i \equiv \frac{\boldsymbol{x}_i - \boldsymbol{C}}{|\boldsymbol{x}_i - \boldsymbol{C}|}. \tag{3}$$

Here $\boldsymbol{x}_i$ and $\boldsymbol{C}$ are the position vectors of agent i and the center of the play area, and $\boldsymbol{e}_i$ is the unit vector indicating the direction from $\boldsymbol{C}$ to $\boldsymbol{x}_i$. The symbol | | indicates taking the absolute value of the vector. We assume that $\boldsymbol{F}_i^s$ is exerted on agent i only when he or she is outside the circle around $\boldsymbol{C}$ with radius L_s. Here L_s is the range of the spatial force. The centripetal nature of $\boldsymbol{F}_i^s$ in the present model originates from experimental data displayed in Fig. S1 (Supplemental Material [26]); it demonstrates that the offensive players showed a circular trajectory. The magnitude of $\boldsymbol{F}_i^s$ linearly increases with the distance between $\boldsymbol{x}_i$ and $\boldsymbol{C}$ [Fig. 2(b)], indicating the effect of a spatial constraint on the positions of agents surrounded by the boundary line of the play area [Fig. 7(b)].

Second, the avoiding force $\boldsymbol{F}_i^a$ is defined by

$$\boldsymbol{F}_i^a = \begin{cases} k_a(|\boldsymbol{x}_i - \boldsymbol{x}_D| - L_a)\boldsymbol{e}_{iD}, & \text{if } |\boldsymbol{x}_i - \boldsymbol{x}_D| \leqslant L_a, \\ \boldsymbol{0}, & \text{otherwise} \end{cases} \quad (4)$$

with the unit vector, $\boldsymbol{e}_{iD} \equiv \frac{\boldsymbol{x}_i - \boldsymbol{x}_D}{|\boldsymbol{x}_i - \boldsymbol{x}_D|}$; position vector of the *Defender*, $\boldsymbol{x}_D$; and force range, L_a. This avoiding force acts on agent i only when he or she is inside the circular range of the *Defender*, characterized by L_a. The magnitude of $\boldsymbol{F}_i^a$ linearly decreases with the distance between $\boldsymbol{x}_i$ and $\boldsymbol{x}_D$, indicating the effect of psychological pressure from the position of the *Defender* [Fig. 2(c)].

Finally, the cooperative force $\boldsymbol{F}_{ij}^c$ is defined by

$$\boldsymbol{F}_{ij}^c = -k_c(|\boldsymbol{x}_i - \boldsymbol{x}_j| - L_c)\boldsymbol{e}_{ij} \quad (5)$$

with the unit vector $\boldsymbol{e}_{ij} \equiv \frac{\boldsymbol{x}_i - \boldsymbol{x}_j}{|\boldsymbol{x}_i - \boldsymbol{x}_j|}$. This force acts on agents i and j as attractive or repulsive, depending on the distance between them [Fig. 2(d)]. The validity of our introducing $\boldsymbol{F}_{ij}^c$ follows the empirical data that show experienced offensive players tend to maintain their equilateral triangle formation throughout the task. The definition of L_c, the characteristic length of the equilateral triangle, will be further discussed in an appendix.

B. Simulation results

In the actual simulation, we systematically examined how the variation in the social force's strength (characterized by the parameters k_c, k_s, and k_a) exerts an influence on the synchronized behavior of the offensive players. The players' motion was simulated by applying the Euler method to Eq. (1) with a time-step size of 0.033 sec. One simulation trial covered 100 sec; 50 trials were performed for a particular set of the parameter values of k_c, k_s, and k_a. All simulations were conducted using MATLAB version R2017b. The paired t-test was used in statistical analyses.

Figure 3 shows the occurrence frequency of the two synchronized patterns, R and PA, for various parameter conditions with respect to k_c, k_s, and k_a. The synchronized patterns R and PA were detected by analyzing the phase difference between two of the three time-series data of the inner angles; comparing the horizontal positions of local maxima and minima in two data, we determined the type of synchronization in accordance with the criteria shown in the bottom panels in Fig. 1(c) [27]. We see from Fig. 3(a) that when all the three parameters are equalized and less than 80.0 N/m, the frequency of the R pattern becomes significantly lower than the PA pattern. This tendency is similar to that observed in the synchronized dynamics of real novice players. On the other hand, when the parameters are collectively set to be 120 N/m or larger, the frequency of the R pattern exceeds significantly that of the PA pattern. This result is consistent with the experimental observation for experienced players. We point out that the threshold of the social force parameters above mentioned, i.e., 120 N/m, is very close to the value estimated from the actual motion of experienced players with body

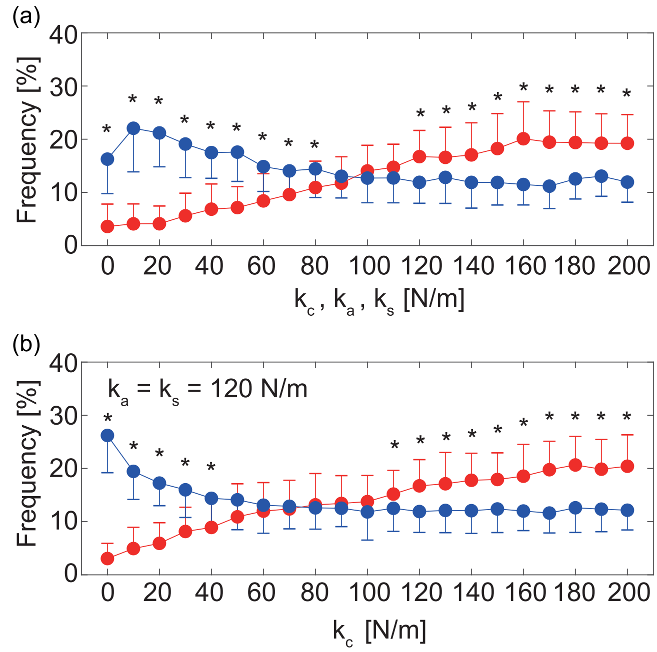

FIG. 3. Occurrence frequency of the two synchronized patterns (red: rotation pattern, blue: partial antiphase pattern) as a function of the force parameters: (a) all the three force parameters (k_s, k_a, and k_c) were equalized and changed, collectively; (b) only the cooperative force parameter k_c was changed, while k_s and k_a were fixed at 120 N/m. Dots and error bar indicate the mean and standard deviation of 50 simulation trials, respectively. Asterisks represent the significant difference between the frequency of R and PA pattern ($p < 0.01$).

mass of $m = 65$ kg more or less. In fact, we experimentally observed that experienced players tend to move in reality with an acceleration of ca. 1.3 m/sec^2 immediately after he or she perceives changes in interpersonal distance, as demonstrated in the Supplemental Material [26] [Fig. S2(D)]; these imply the possibility that experienced players are driven by social forces with the strength of ca. 120 N/m, though it is not yet clarified what kinds of social forces among the three candidates would be most responsible for the high-occurrence frequency of the R pattern.

Figure 4 provides us further insight into the role of the social forces; it shows how the synchronized motion of the offensive players depends on the presence or absence of the three classes of social forces. All the three force parameters were set to 120 N/m in Fig. 4(a), while one of the three parameters was artificially set to zero in Figs. 4(b)–4(d). Particular attention should be paid to the following two cases: (1) When all the three parameters are active [Fig. 4(a)], then the time evolution of the player's inner angles (left panel) and the histogram of the angles for 50 trials (right panel) are both similar to the empirical data of real experienced players. (2) When the cooperative force $\boldsymbol{F}_i^c$ was eliminated [Fig. 4(b)], the simulation data became similar to the motion exhibited by real novice players in behavioral experiments. The contrasting observation in Figs. 4(a) and 4(b) suggests that the cooperative force is a keystone for realizing the excellent team coordination in the three versus one ball possession task. Supporting data are given in Fig. 3(b), which provides the k_c dependence of

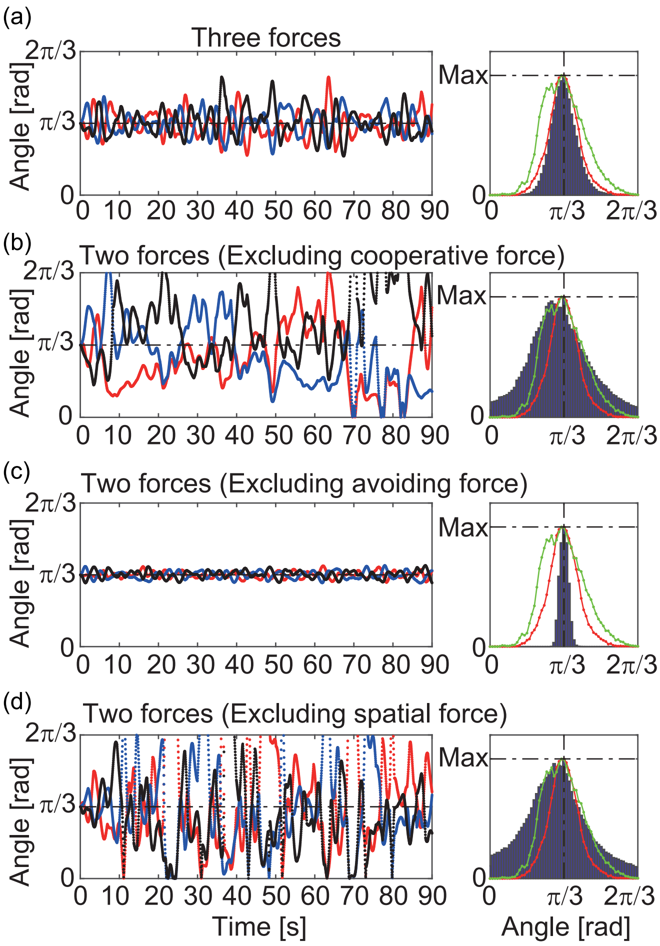

FIG. 4. (Left) Time series of the three inner angles. The model used in the simulation involves: (a) all three social forces ($k_s = k_a = k_c = 120$ N/m), (b) two social forces excluding the cooperative force ($k_c = 0$, $k_s = k_a = 120$ N/m), (c) two forces without the avoiding force ($k_a = 0$, $k_s = k_c = 120$ N/m), and (d) two without the spatial force ($k_s = 0$, $k_a = k_c = 120$ N/m). (Right) Frequency of the three inner angles for 50 trials. The red and green curves represent the inner angle distribution associated with experienced and novice players, respectively, deduced from empirical data.

the occurrence rate of the two synchronized patterns: R and PA, under the condition that $k_a = k_s = 120$ N/m. It is clearly seen that the rate of the PA pattern (R pattern) dominated at small (large) k_c. In addition, the two curves in Fig. 3(b) monotonically increased or decreased with k_c, showing a crossover at an intermediate value of k_c. These results mean that the cooperative force among teammates plays a fundamental role in determining the degree of team coordination.

It is important to note that the simulation data shown in Figs. 4(c) and 4(d), in which $\boldsymbol{F}_i^a$ and $\boldsymbol{F}_i^s$ are respectively omitted, cannot practically describe a real player's performance. In the case of $\boldsymbol{F}_i^a = \boldsymbol{0}$ [Fig. 4(c)], for instance, the three offensive agents did not at all react to the movement of the *Defender*; therefore, the equilateral triangular formation persisted with only a slight perturbation. At first glance, the condition of $\boldsymbol{F}_i^a = \boldsymbol{0}$ may seem to be analogous to the situation in which the motion of offensive players is much quicker than that of the defensive player. But this was the case only when $\boldsymbol{F}_i^a = \boldsymbol{0}$ in principle. We confirmed that, as far as $\boldsymbol{F}_i^a$ is active, the preference of the R mode for experienced players is fairly rigid against the change in the agility of *Defender* [see Fig. S3(A) in the Supplemental Material [26]]. The case of $\boldsymbol{F}_i^s = \boldsymbol{0}$ [Fig. 4(d)] is also unrealistic, because the three agents took no notice of the circular boundary and thus moved too far outside the designated playing area. The unbounded motion of players associated with Fig. 4(d) as well as those for Figs. 4(a)–4(c) can be found in the Supplemental Movie [26].

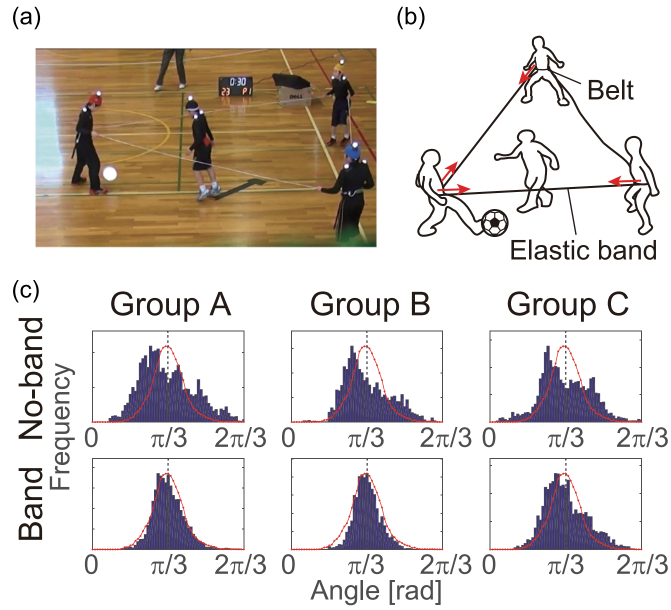

FIG. 5. (a) Snapshot of guidance tool-based experiment performed by novice players. (b) Schematic diagram of physical guidance tool. (c) Frequency of the three inner angles across four trials of 60 seconds, without (upper) and with (lower) the use of the elastic band. The red curves demonstrate the distribution pattern exhibited by experienced players, duplicated from Fig. 4.

C. Guidance tool to perceive cooperative forces

To examine the validity of our speculation that the cooperative force is indispensable to realizing high performance, we developed a physical guidance tool that facilitates players' perceptions of the cooperative force. We then applied it to novice players who were elementary school students [Fig. 5(a)]. This tool is composed of three long elastic bands of an equal length and three waist belts. The belt and band are alternately connected, forming a triangular configuration [Fig. 5(b)]. In the verification experiment, three offensive players wore the belts, and the other player was instructed to play the role of the defense. The elastic bands created a lateral tensile force between two adjacent offensive players when they were far apart, making them aware that they should be closer to each other to achieve high performance. Conversely, when two offensive players' distance from each other was shorter than the natural length of bands, the bands were slacked, making them aware that they should step away from each other.

We experimentally confirmed that the guidance tool provides an *effective* cooperative force, thus drastically improving the degree of synchronized motion in novice players. The results are summarized in Fig. 5(c). When the tool was not in use, the inner angle distribution significantly deviated from that exhibited by experienced players, as indicated by the red curves in the graphs. Once the tool was in use, the distribution became similar to that of experienced players, evidencing that sustained attention towards teammates, represented by the cooperative force, is crucial for a team to attain experienced team coordination in the ball possession task. It is necessary to note that the guidance tool yielded almost no improvement in an individual's ball manipulation skill. In fact, the total number of successful passes performed by novice players remained largely unchanged even when they used the guidance tool. This was confirmed by the permutation test ($p = 0.79$); see Table S1 in the Supplemental Material [26].

IV. CONCLUDING REMARKS

In the present work, we focused on synchronized behavior in a three versus one ball possession task to obtain insight into the fundamental skills required for excellent team coordination. Considering the empirical data, we developed a theoretical model involving three types of social forces and demonstrated that the model describes a real player's movement. The agreement between the simulated results and experimental measurements indicates that the cooperative force, which quantifies the degree of individual player's attention to teammates, is the fundamental social skill needed to realize experienced team coordination. Simply put, what makes experienced players able to harmonize their movements is a broad view and good anticipation. In fact, it is widely accepted in the field of sports science that experienced players frequently observe the positions and movements of other players, also known as "off the ball" skills [28]. Our results suggest that the social force-based approach works well for studying the effect of invisible skills on the collective dynamics of players.

We also demonstrated that the physical guidance tool is useful for improving the team coordination of novice players. The tool helps them perceive changes in interpersonal distance and react to it as if they were driven by the cooperative force in our social force model. This result opens avenues to develop new physical education materials; that is, for a given collective sport, we can identify the fundamental social skill by first establishing the social force model and then developing a guidance tool that supports the perception of interpersonal or environmental information, as the model suggests.

As a final note, animal societies perform a wide variety of self-organized collective behavior, such as nest-building behavior by ants [29,30], coordinated movement of fish schools against predatory attacks [31], and defensive behavior in honeybees [32]. Exposed to the struggle for survival, individuals in animal societies are likely to fulfill excellent team coordination in a self-organized manner. In this context, social force-based approaches will provide clues to understanding what kind of perceived information drives the optimal (sometimes synchronized) motion of individuals.

ACKNOWLEDGMENTS

We thank A. Kijima, T. Hirakawa, K. Kadota, and M. Nakayama for their inspiring discussions, D. Suzuki for his help in developing the guidance tool, and K. Hamano for assistance in performing the experiment. This work was supported by JSPS KAKENHI Grants No. 16K16518, No. 17H02141, and No. 24240085.

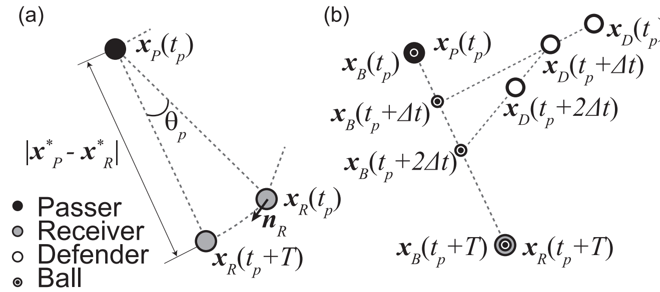

FIG. 6. (a) Diagram of *Receiver*'s position and movement. (b) Diagram of the *Defender*'s position and movement relative to the ball's trajectory.

APPENDIX A: *RECEIVER* AND *DEFENDER* MOVEMENT

It was assumed that the *Receiver* moves in a uniform circular motion defined by

$$\frac{d\boldsymbol{x}_R}{dt} = \frac{|\boldsymbol{x}^*_P - \boldsymbol{x}^*_R|}{T}\theta_p \boldsymbol{n}_R. \tag{A1}$$

Here we used the notation $\boldsymbol{x}^*_i \equiv \boldsymbol{x}_i(t_p)$ with t_p being the moment at which the *Passer* releases a ball to the *Receiver*. The *Receiver* moves along the circle with radius $|\boldsymbol{x}^*_P - \boldsymbol{x}^*_R|$ about the origin $\boldsymbol{x}^*_P$ [Fig. 6(a)]. Equation (A1) states that the *Receiver* runs from the starting point, $\boldsymbol{x}^*_R$, to the final point, $\boldsymbol{x}_R(t_p + T)$, with a constant speed in the time duration T. $\boldsymbol{n}_R$ is the unit tangent vector whose direction changes at every moment, as illustrated in Fig. 6(a). The ball moves in a uniform linear motion with a speed of $\frac{|\boldsymbol{x}^*_P - \boldsymbol{x}^*_R|}{T}$.

The *Defender* moves at a constant speed defined by

$$\frac{d\boldsymbol{x}_D}{dt} = \frac{d_D}{T}\boldsymbol{e}_D, \tag{A2}$$

where d_D is the moving distance of the *Defender* per pass. $\boldsymbol{e}_D$ is the unit vector defined by $\frac{\boldsymbol{x}_B(t+\Delta t) - \boldsymbol{x}_D(t)}{|\boldsymbol{x}_B(t+\Delta t) - \boldsymbol{x}_D(t)|}$, where $t = t_p + n\Delta t$ with n being an integer. Figure 6(b) indicates that the *Defender* changes its moving direction at every moment, while the ball moves straight ahead.

APPENDIX B: MODEL PARAMETERS

The parameters used in the present social force model are summarized in Table I. Our definitions of these parameters were based on either the measurement values for each parameter in the experiments or theoretical consideration of equilibrium positions of players, as explained below.

The agent's mass m was set to be the mean value for all participants in the experiment ($m = 65$ kg). The length of the play area L was defined on the basis of the experimental setting ($L = 6.0$ m).

The time interval of passes T, pass angle θ_p, and the moving distance of the *Defender* per pass d_D showed large fluctuations in an actual player's performance (Fig. S2). In the simulation, T was defined as a uniform random parameter, while the latter two were constant parameters. Essential data for the definitions

TABLE I. Simulation parameters.

Parameter	Symbol	Value	Unit
Agent's mass	m	65	kg
Interpass interval	T	0.5–1.5	sec
Pass angle	θ_p	3.0	deg
Moving distance of *Defender* per pass	d_D	2.0	m
Size of square play area	L	6.0	m
Cooperative range	L_c	$3\sqrt{3}$	m
Spatial range	L_s	2.0	m
Avoiding range	L_a	4.0	m

were video footage of an experienced player's performance, in which 1049 passes were recorded. We then examined the distribution of T obtained from the data and approximated it as the uniform random distribution within the range of 0.5–1.5 sec, in accordance with the data showing a mean value of $M = 1.0$ sec and standard deviation of SD $= 0.5$ sec [Fig. S2(A)]. Meanwhile, θ_p and d_D were set to be the mean of the distribution of all passes experimentally observed [Figs. S2(B) and S2(C), $\theta_p = 3.0^\circ$, $d_D = 2.0$ m].

The definitions of the range parameters L_c, L_a, and L_s relied on the conjecture as to equilibrium positions of players. It was first assumed that in an equilibrium state, the *Defender* was positioned at the center of the square-shaped play area, and the three offensive agents were located at the vertices of an equilateral triangle, in which all three social forces were inactive. More precisely, the triangle is inscribed in a circle, and the circle is inscribed in a square-shaped play area with the linear dimension L [see Fig. 7(a)]. In the equilibrium state, the cooperative force $\boldsymbol{F}_i^c$ is supposed to vanish and the other two forces, $\boldsymbol{F}_i^s$ and $\boldsymbol{F}_i^a$, counterbalance each other. As a consequence, L_c is defined as

$$L_c = \frac{\sqrt{3}}{2}L, \tag{B1}$$

as follows from Fig. 7(a). In addition, the equilibrium condition of $\boldsymbol{F}_i^s$ and $\boldsymbol{F}_i^a$ implies the relationship of

$$\frac{L}{2} - L_s = L_a - \frac{L}{2} = l, \tag{B2}$$

where l is an undetermined parameter. It is reasonable to set the value of l as 1 m, because in the experiment, one step (approximately 1 m) is a threshold distance over which the players feel caution when approaching the *Defender* or departing from the center of the play area.

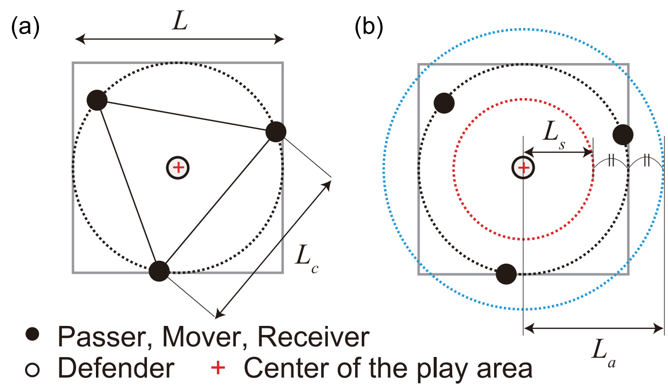

FIG. 7. (a) Schematic definition of the cooperative range parameter L_c. (b) Definition of the avoiding range parameter L_a and spatial range parameter L_s.

We should note here that, although the specific values listed in Table I were used primarily in our simulations, the main conclusion depends less on the choice of the values. For instance, the occurrence frequency of the R (and PA) pattern was found to be largely insensitive to the change in d_D and L, as demonstrated in the Supplemental Material [26] [Fig. S3].

APPENDIX C: EXPERIMENTAL SETUP OF GUIDANCE TOOL

A total of 12 elementary school students (9–14 years old) participated in the experiment as novice players. They were separated into three groups according to their grade level in school and skill level in team sports. The experimental protocol was approved by an institutional ethics committee in Kogakuin University, Japan, and conformed to the principles expressed in the Declaration of Helsinki. Each group played six trials of the three versus one ball possession task for 60 sec under the following two different conditions. In the first three trials, the task with the guidance tool was conducted with players; each player wore waist belts connected by two elastic bands with a natural length of 4 m. In the remaining three trial, they performed the usual ball possession task without the tool. In all six trials for each group, the time-varying positions of the players on the ground were captured by four optical motion capture cameras at 120 Hz (OptiTrack Prime 17W, NaturalPoint Inc., Corvallis, OR, USA).

[1] H. Ulrich and G. J. B. Probst (eds.), *Self-organization and Management of Social Systems: Insights, Promises, Doubts, and Questions* (Springer-Verlag, Berlin, 1984).

[2] R. R. Vallacher and A. Nowak (eds.), *Dynamical Systems in Social Psychology* (Academic Press, San Diego, 1994).

[3] J. C. Gorman, T. A. Dunbar, D. Grimm, and C. L. Gipson, Front. Psychol. **8**, 1053 (2017).

[4] A. Kijima, K. Yokoyama, H. Shima, and Y. Yamamoto, Eur. Phys. J. B **87**, 41 (2014).

[5] R. da Silva, M. H. Vainstein, S. Gonçalves, and F. S. F. Paula, Phys. Rev. E **88**, 022136 (2013).

[6] L. C. Malacarne and R. S. Mendes, Physica A **286**, 391 (2000).

[7] R. N. Onody and P. A. de Castro, Phys. Rev. E **70**, 037103 (2004).

[8] S. D. Silva, R. Matsushita, and E. Silveira, Physica A **392**, 5376 (2013).

[9] Z. Yue, H. Broich, F. Seifriz, and J. Mester, Stud. Appl. Math. **121**, 223 (2008).
[10] Z. Yue, H. Broich, F. Seifriz, and J. Mester, Stud. Appl. Math. **121**, 245 (2008).
[11] J. Duch, J. S. Waitzman, and L. A. N. Amaral, PLoS ONE **5**, e10937 (2010).
[12] Y. Yamamoto and K. Yokoyama, PLoS ONE **6**, e29638 (2011).
[13] K. Fujii, K. Yokoyama, T. Koyama, A. Rikukawa, H. Yamada, and Y. Yamamoto, Sci. Rep. **6**, 23911 (2016).
[14] K. Yokoyama and Y. Yamamoto, PLoS Comput. Biol. **7**, e1002181 (2011).
[15] A. Takamatsu, R. Tanaka, H. Yamada, T. Nakagaki, T. Fujii, and I. Endo, Phys. Rev. Lett. **87**, 078102 (2001).
[16] K. Okamoto, A. Kijima, Y. Umeno, and H. Shima, Sci. Rep. **6**, 36145 (2016).
[17] M. Golubitsky and I. Stewart, *The Symmetry Perspective: From Equilibrium to Chaos in Phase Space and Physical Space* (Birkhäuser, Basel, 2002).
[18] D. Helbing and P. Molnár, Phys. Rev. E **51**, 4282 (1995).
[19] R. C. Schmidt and M. J. Richardson, in *Coordination: Neural, Behavioral and Social Dynamics*, edited by A. Fuchs and V. K. Jirsa (Springer, Berlin, 2008), pp. 281–308.
[20] O. Oullier, G. C. de Guzman, K. J. Jantzen, J. Lagarde, and J. A. S. Kelso, Social Neurosci. **3**, 178 (2008).
[21] J. Jiang, B. Dai, D. Peng, C. Zhu, L. Liu, and C. Lu, J. Neurosci. **32**, 16064 (2012).
[22] K. Lewin, *Field Theory in Social Science* (Harper Torchbooks, New York, 1964).
[23] D. Helbing, I. Farkas, and T. Vicsek, Nature (London) **407**, 487 (2000).
[24] W. J. Yu, R. Chen, L. Y. Dong, and S. Q. Dai, Phys. Rev. E **72**, 026112 (2005).
[25] M. Chraibi, A. Seyfried, and A. Schadschneider, Phys. Rev. E **82**, 046111 (2010).
[26] See Supplemental Material at http://link.aps.org/supplemental/10.1103/PhysRevE.97.022410 for additional information using figure, table, and a movie.
[27] When neither R or PA was detected, the offensive agents showed random motion or fell into the partial in-phase (PI) synchronized pattern as found in Ref. [14]. Among them, our focus was paid in the model analysis to the two patterns R and PA, because they are what we observed in real-world player's motion and are believed to characterize the collective motion performed by experienced and novice teams, respectively.
[28] A. M. Williams, K. Davids, and J. G. Williams, *Visual Perception & Action in Sport* (Routledge, New York, 1999).
[29] P. N. Kugler and M. T. Turvey, Human Movement Sci. **7**, 97 (1988).
[30] N. R. Franks and J.-L. Deneubourg, Anim. Behav. **54**, 779 (1997).
[31] J. K. Parrish, S. V. Viscido, and D. Grünbaum, Biol. Bull. **202**, 296 (2002).
[32] J. Millor, M. Pham-Delegue, J. L. Deneubourg, and S. Camazine, Proc. Natl. Acad. Sci. USA **96**, 12611 (1999).